4

Calibration of Locket

In Chapter 3 we have seen the hardware details and specifications of the *locket* which we have used for acquisition of ECG signals. Here we reproduce some of the important features and measured performance parameters of the analog processing part of the *locket* in Table 4.1 (from [117]) for convenience.

Table 4.1. Specifications of the analog processing part of the *locket*. Reproduced from [117].

Feature/Parameter	Value
ECG-lead	Single, primary lead
Battery Voltage	3.7V
Supply current for a single-channel	22μA
Voltage gain	600
Input voltage dynamic range	6mV
Input referred noise voltage (rms)	6μV (0<BW<200Hz)
Common mode rejection ratio	100dB (at 60Hz)
Output signal slew rate	50mV/μs
Input impedance	3.2MΩ
High-pass cut-off frequency	0.05Hz
Low-pass cut-off frequency	106Hz
Quantization	12 bits/sample in the range 0-2.5V
Memory	32MB SD card
File formates	binary, ASCII
Computer interface	serial port data transfer, on-line and off-line

The battery voltage 3.7V matches with the commercially available Li-ion rechargeable, BL-5C battery. The supply current specification gives an idea how frequently the battery needs to be recharged. For example, the BL-5C battery permits the *locket* to record single channel ECG data continuously for more than 10 hours. The voltage gain is set to amplify the analog signal captured by the electrodes sufficiently for analog to digital conversion. For the

S. Chaudhuri et al., *Ambulation Analysis in Wearable ECG*, DOI: 10.1007/978-1-4419-0724-0_4, 45

specified operating voltage and gain the amplifier is able to cover the dynamic range of 6mV, which is considered suitable for surface ECG. Typically, the ECG signal has an amplitude of 1mV at the skin surface but it can be as high as 3mV for some subjects. The rms level of noise is as low as 6μV as indicated in Table 4.1, which accounts for the thermal noise of resistors at the input of the amplifier. The common mode rejection ratio indicates capability of the amplifier to reject the common mode input signal such as powerline noise. The slew rate represents the highest rate of change in the input signal and hence the maximum amplitude of the signal at a specified frequency that the amplifier can handle. The input impedance of the amplifier matches with the skin electrode impedance for optimal capture of the ECG signal from the skin surface. The highpass and lowpass cut-off frequencies determine the frequency range of the amplifier and the selected bandwidth is considered suitable for the ECG signal for clinical applications.

The detailed specifications of the *locket* related to the analog part such as frequency response, noise level, common mode rejection ratio, slew rate, etc., have been characterized and reported in [117]. However, the sampling rate which is determined from the crystal frequency and the multiplier set in the firmware, is adjustable. This is preferred over a fixed sampling rate to suit the needs of different applications and limitations imposed by the number of channels and the available memory storage, particularly at the development stage of the recorder. For the prototype used in this work the sampling rate is pre-set and kept the same for all data recorded for the same purpose.

In this chapter we discuss a simple calibration procedure performed to confirm the pre-set sampling rate of the *locket* with respect to a standard analog to digital converter (ADC). The sampling rate is useful when the ECG signal is required to be analyzed with respect to other signals such as accelerometer data.

4.1 Calibration Requirements

It is important to know the sampling rate for physical understanding and interpretation of the signals recorded in digital form. The sampling rate can provide the exact time instance of a particular event in the digital signal and also allows us to compare the signals from several different sensors working at different sampling rates. For example, in Chapter 8 we use body acceleration signals recorded using a stand-alone motion sensor system with a sampling rate different from that of the *locket*. Thus the collected acceleration and ECG signals are at different sampling rates. To analyze the ambulation activities in time we must have a common time reference for both the signals which is possible only if the sampling rates for both the systems are known.

A pulse with a very stable amplitude, frequency and duty cycle is required as the input for the calibration of the sampling rate of the *locket*. The number of samples during ON time of the pulse can be counted to know the exact

sampling rate. There are, however, some limitations on the calibration pulse: the amplitude of the pulse should be less than 1mV in order to prevent the device from going into saturation due to high amplifier gain and the ON time of the pulse should be integer multiple of sampling period to avoid the error in counting of number of samples per second. Considering the difficulties in generating the calibration pulse with the strict specifications for the method given above, we instead show here a practical approach to estimate or confirm the exact sampling rate of the *locket* with an analog to digital converter (ADC). In this method we require an analog ECG processor (amplifier) and an ADC with known sampling rate. We use the powerline interference as a reference signal for both the systems, the *locket* and the ADC.

4.2 Experimental Set-up

Since we wish to use the powerline signal as a common reference signal for the ADC as well as the recorder to be calibrated, we allow the powerline interference to occur in both the channels. It is known that there is increased powerline interference if the lead cables of the ECG amplifiers are not shielded [137]. Therefore, for the signal acquisition process during the calibration, we use unshielded cables and choose an environment like an electronics laboratory, where significant powerline interference is known to occur. Care has to be taken that the level of the interference signal does not saturate the ECG amplifier. This is practically achieved by keeping an appropriate distance from the source of the interference like a switch or a power supply regulator. This method is different from the impedance measurement using a current supplied across the electrode at a specified frequency, since there is no active source connected to the electrode itself. Since the skin electrode impedance is sensitive to the skin stretch at the lower frequencies (below 200Hz) [40], we restrict any body movements activity (BMA) during the ECG acquisition to prevent undesired artifacts. Thus according to the model given in Eq. (1.1) of the recorded ECG signal, $r(n) = q(n) + s(n) + \eta(n)$, we try to enhance the sensor noise $\eta(n)$ with the characteristic of a very narrow spectrum, centered at $\approx$50Hz in this experiment, while minimizing the motion artifact signal $s(n)$. Ideally, $s(n) = 0$ in absence of any BMA. A set-up of the experiment is given in Fig. 4.1, in which two parallel channels of the lead-II ECG acquisition are depicted. The two channels for the lead-II configuration are obtained by placing a pair of electrodes side-by-side with a separation of 1.5cm, for each of the paired locations as shown in Fig. 4.1. The upper channel is connected to an ECG amplifier followed by an ADC, *NI-USB-6009* from *National Instruments (NI)*. The *NI-USB-6009* is configured to sample the analog signal in the single ended mode with a common ground (the same as the amplifier ground), unity gain and quantization of 12 bits/sample. Further details about connections and configuration of *NI-USB-6009* are provided in [1]. The digitized data is transferred to the computer through a universal serial bus (USB) in real-time

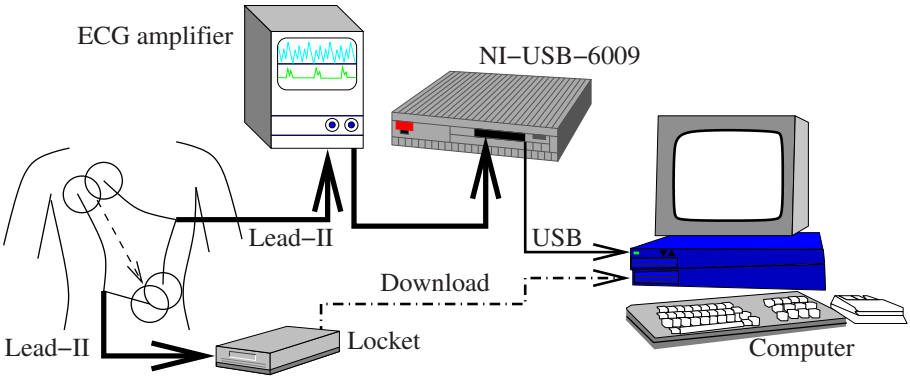

Fig. 4.1. Experimental set up for the calibration of the sampling frequency of the wearable ECG recorder.

using a software interface. The sampling frequency of the device was software controlled using the *NI-DAQmx Base 1.4* driver programmed through the *NI Labwindows CVI 7.1* interface. The other channel in Fig. 4.1, is connected to the *locket*. Since the data in both the channels are being recorded separately without any time synchronization, the recordings in both the channels are started with a minimum possible delay between the two channels.

4.3 Calibration Technique

From the experimental set-up described in the previous section, we have seen that there are two ECG signals recorded separately but from the same location configured for the lead-II: one using the *locket* and the other using the ADC (*NI-USB-6009*). Let us denote the recorded signal in *locket* as x_1 and that recorded in the ADC as x_2. Let the sampling rates of the signals x_1 and x_2 be f_1 and f_2, respectively. Here f_1 is unknown and f_2 is pre-programmed in the ADC using the software.

It is known that the powerline interference is dominant in both the recorded signals, which is centered at a frequency $\approx$ 50Hz. However, the exact value of the frequency f_p may deviate by $\pm$2Hz. Moreover, the value of f_p may not remain steady over a long period of time. Thus we cannot adopt the method of counting the number of samples per cycle of the interference wave for calculating the sampling rate. Instead, we acquire a reference signal using an ADC for which the sampling rate is known. Here, we use the fact that both the ADC and the *locket* signals are being recorded simultaneously, hence the line frequency f_p remains the same for both the signals. A block diagram of the processing steps involved in this method is given in Fig. 4.2. First, in the DFT block the magnitude spectrum of the input signal is computed over a fixed window using discrete Fourier transform (DFT). Since the frequency

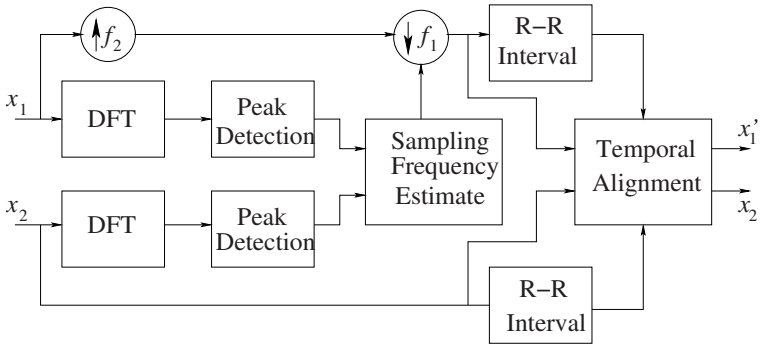

Fig. 4.2. Processing steps in the calibration method.

resolution of the DFT is related to the number of samples in the window as well as the sampling rate, we should choose a reasonably high number of samples. The powerline frequency component is dominant in both the signals x_1 and x_2 and hence it produces corresponding peaks in the computed spectra. Since f_1 is unknown, the locations of the peaks are detected on a normalized frequency axis $2f_O/f_2$, where f_O is frequency observed in the DFT at the sampling rate of f_2. Therefore, f_O is the actual frequency for x_2, whereas the actual frequency for x_1 is given by $(f_O f_1)/f_2$. The unknown sampling frequency f_1 is estimated in Fig. 4.2 as follows.

Let us denote the locations of the peaks on a normalized frequency axis $2f_O/f_2$ as p_1 and p_2 for the signals x_1 and x_2, respectively. The actual powerline frequency f_p corresponding to both the peaks is the same. However, the observed frequency f_O is related to the actual frequency in each signal in a different way as explained above.

Therefore we have,

$$\begin{aligned} f_p &= \tfrac{p_1}{2}\ \tfrac{f_1}{f_2} = \tfrac{p_2}{2} \\ \Rightarrow \quad f_1 &= f_2 \tfrac{p_2}{p_1}. \end{aligned} \tag{4.1}$$

Since we know the variables in the right hand side of the above equation, we can calculate the sampling frequency of the *locket* f_1. We can also calculate the powerline frequency f_p for the given data.

4.4 Results and Discussion

Following the technique given in the above section, the magnitudes of DFT (spectra) of the signals x_1 and x_2 against normalized frequency values $2f_O/f_2$ are plotted in Fig. 4.3(a), where $f_2 = 256$Hz. A distinct peak in the spectrum of each of the signals is found as shown in Fig. 4.3(a), which is attributed to the powerline interference. However, the locations of the peaks in both the

spectra are shifted because of difference in the frequency scales for both the signals. The shift is more clearly visible in the cross-correlation function of the two spectra, plotted in Fig. 4.3(b). The half-width of the lobe produced in the cross-correlation represents the variance in the frequency estimation, which is < 0.2Hz. We have found the values of $f_1 = 242$Hz and $f_p = 48.9$Hz using Eq. (4.1) from the recorded data in this experiment.

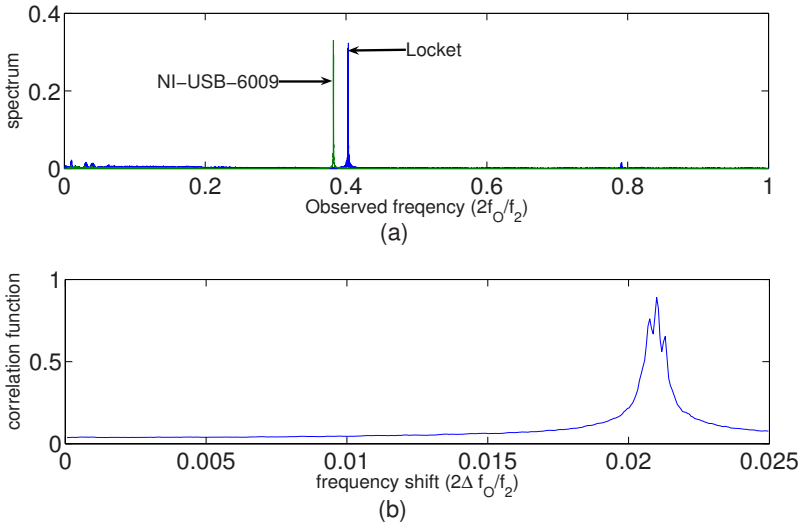

Fig. 4.3. (a) Observed spectra of powerline interference with sampling rate f_2=256Hz and unknown f_1. (b) The shift in the observed powerline frequencies using cross-correlation of the two spectra.

It is worth explaining here, why the cross-correlation based technique should work in estimating the sampling frequency of the locket. Ideally, spectra of both the signals x_1 and x_2 are nearly identical as both are acquired from (almost) the same lead-II positions of the ECG electrodes. The difference in peak in Fig. 4.3(a) is due to different choice of sampling frequencies in two channels. Ideally, one would like to dilate or contract one of the power spectral densities (PSD) to estimate the exact frequency. Since we have selected the reference frequency f_2, very close to the locket frequency f_1, the expression Eq. (4.1) can be simplified as

$$\begin{aligned} f_1 &= f_2 \frac{p_2}{p_1} \\ &\approx f_2 \frac{p_1+\delta}{p_1} \\ &\approx f_2 + \frac{\delta}{p_1} f_2 \end{aligned}$$

$$\approx f_2 + \Delta f, \tag{4.2}$$

where Δf is the shift in frequency. Cross-correlation of the PSD of these two signals, thus, gives us the frequency offset required to calculate the sampling frequency of the locket.

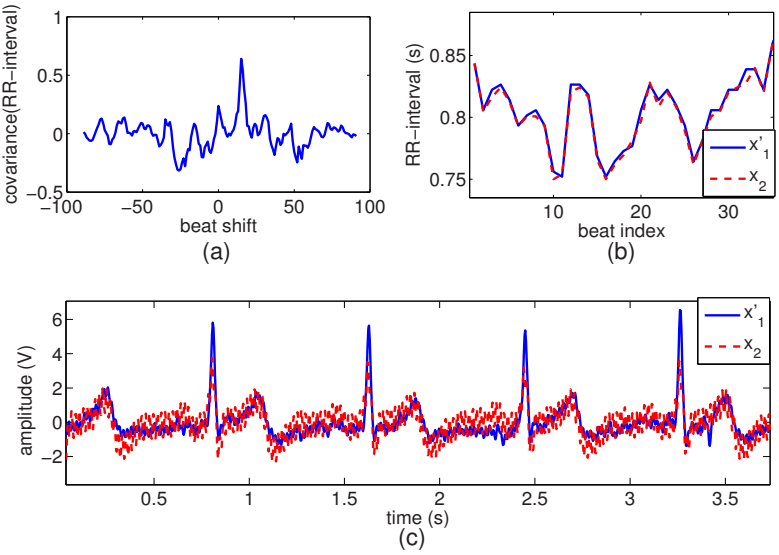

Fig. 4.4. Temporal synchronization of the two signals using the covariance of RR interval sequence. (a) Cross-covariance function of the two RR interval sequences, (b) the two RR interval sequences after alignment and (c) the ECG signals after alignment.

Now, the sampling rate of the *locket* is known, which can be used for resampling of the signal x_1 so as to match it with the sampling rate of x_2. The signal x_1 is resampled by a rational factor of f_2/f_1 as indicated by $\uparrow f_2$ (upsampling) followed by $\downarrow f_1$ (down sampling) in Fig. 4.2. Let us denote the resampled version of signal x_1 as x_1'. The resampled signal x_1' and the signal x_2 have the same sampling rate but they may not be exactly time-synchronized. At this stage we cannot use cross-correlation between these two signals for time-synchronization because the powerline noise as well as ECG signal are both periodic in nature and may produce several peaks in the cross-correlation function creating ambiguity in finding the exact delay between the two signals. Instead, we use the cross-covariance function of RR interval obtained from QRS detection in both x_1' and x_2. We also verify that the error between the corresponding pairs of RR interval values for both the signals is very small after time synchronization. The cross-covariance function of the RR interval series is shown in Fig. 4.4(a). A distinct peak at a shift of

16 beats indicates the delay between the two signals. A part of RR intervals for both the signals after the alignment is shown in Fig. 4.4(b), indicating a perfect match. The ECG signals after time-synchronization are shown in Fig. 4.4(c). The spectra of both the signals are shown in Fig. 4.5. At the lower frequency band of 0-25Hz, both the spectra are matching very well, the faster roll-off for spectrum of signal x_2 is due to the 50Hz high frequency cut-off (as opposed to 106Hz for the *locket*) of the ECG amplifier used in the experiment. The peaks of the powerline are produced at $f_p = 48.9$Hz in both the spectra.

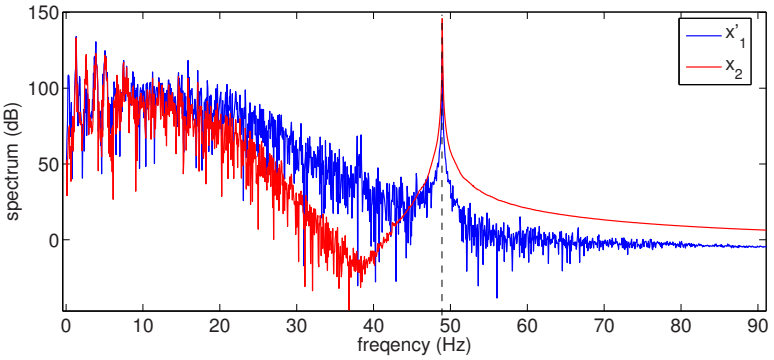

Fig. 4.5. The spectra of two ECG signals after achieving the alignment. The peak at powerline frequency is in perfect alignment for both the signals.

In this chapter, we have presented a simple yet effective method for calibrating the sampling rate of a W-ECG using powerline interference. The experimental set-up for the calibration is very simple to implement in the laboratory. The method is also useful for calculating the exact powerline frequency over a short period of time and hence can be used for generating a reference signal for adaptive noise removal applications. Since the method is based on DFT, peak detection and cross-correlation operations are easy to implement on micro-computers, and hence it can be easily adapted for W-ECG.